eu**spen**'s 18th International Conference &
Exhibition, Venice, IT, June 2018
www.euspen.eu

Numerical modelling and parametric study of grain morphology and resultant mechanical properties from selective laser melting process of Ti6Al4V

Mohamad Bayat[1,*], Sankhya Mohanty[1], Jesper H. Hattel[1]

[1]*Department of Mechanical Engineering, DTU, Lyngby, Denmark*

[*]*mbayat@mek.dtu.dk*

Abstract
In this paper, a transient 3-dimensional thermal model for the selective laser melting process, based on the finite volume method, has been developed, which takes into account the phase change and powder to bulk material transition. A parametric study has been performed for the temperature field as well as the melt pool dimensions, and the results show the impact on melt pool size. Also, in this paper, a straightforward metallurgical model has been coupled to a thermal model, which uses the temperature gradient and the cooling rate on the melt pool borders at the onset of solidification to determine whether the grains have columnar or equiaxed morphology. Furthermore, the effect of process parameters on the size of grains and subsequently the yield stress has been studied via empirical equations. The results show that low speed along with high laser power (higher laser energy density) will cause low cooling rates and prompt the formation of large grain. This would consequently give rise to lower tensile strength, as compared to lower laser energy density where smaller grains are formed due to higher cooling rates.

SLM – Thermal model – Finite volume method – grain morphlogy – parametric study

1. Introduction

Additive manufacturing is currently finding new and growing applications in many industries such as aerospace, medical, automobile, etc. In selective laser melting (SLM), which is a type of powder bed fusion additive manufacturing technique, the process begins when a layer of fine metallic powder (with sizes around 20 to 50 micrometers) is evenly distributed over a solid substrate. After the first layer has been accreted, the laser scans the predefined locations and by selectively melting the powder, the first solid layer is fabricated. After the first layer has been cooled down, the same process is repeated for subsequent layers until the whole metal part is produced.

SLM has many advantages over conventional production methods (e.g. casting and forging), such as lower material waste and faster production speed. However, to compete with existing conventional processes, the quality of its final products need to be more predictable. A straightforward way to predict the effect of process parameters on the parts' quality would be through production of large number of samples. The more elegent way, however, would be via proper numerical modelling that takes into account proper physics and is able to replicate experimental observations.

Literature is abundant in thermal modelling of SLM process. More recently, Li and Gu developed a finite element thermal model for SLM of commercially pure titanium powder [1]. They investigated the effect of laser input power and the scanning speed on the shape and size of the melt pool, as well as its impact on the maximum temperatures formed during the process. Huang et al., studied the effect of SLM process parameters on both the temperature field and morphology of the parts [2], while considering material shrinkage during SLM, and were able to show that ignoring this event would result in lower temperature predictions.

Similair works for heat conduction modelling of SLM can be found in literature for different types of powders, e.g. AISI 316L [3,4], Nitinol [5], W-Ni-Fe [6], Aluminum [7], Inconel 718 [8], Inconel 625 [9]. A number of researchers have also considered the fluid dynamics in thermal models and suggested that neglecting this phenomenon can result in overestimation of the temperature field [10,11].

Apart from the thermal field and its effects on residual stresses and part dimensional accuracy, the microstructure morphology and the crystallographic texture also has a high level of interest, especially for industries where targeted material properties are required. Raghavan et al. studied the impact of the EBM process parameters on the grain morphology of the samples [12]. Bontha et al. also studied the effect of EBM scanning speed and input power on the grain morphology of Ti6Al4V, where they assumed a point heat source for their simulation [13].

In this paper, the effects of the SLM process parameters on the thermal field and melt pool dimension has been studied in detail using a 3D thermal model. Also, a metallurgical model has been developed to predict the grain morphology (equiaxed ot columnar) of the SLM parts, and the subsequent effect on the yield stress and average grain sizes are analysed.

2. Numerical model

The 3D thermal model is based on the conventional heat conduction equation with Newtonian cooling and surface radiation similar to that described by Mohanty and Hattel [14]. The modelled domain of 2 mm by 2 mm by 1 mm is discretized into 97000 elements. A Gaussian heat flux has been imposed on the top surface to resemble the actual laser-powder interaction. The effective value for powder material properties are also considered e.g. the powder specific heat heat capacity (based on a solid density of ρ_{solid} and porosity of φ) is calculated as [7]:

$$c_p = \frac{[1-\varphi]c_{p_{solid}}\rho_{solid} + \varphi c_{p_{air}}\rho_{air}}{[1-\varphi]\rho_{solid} + \varphi\rho_{air}} \qquad (1)$$

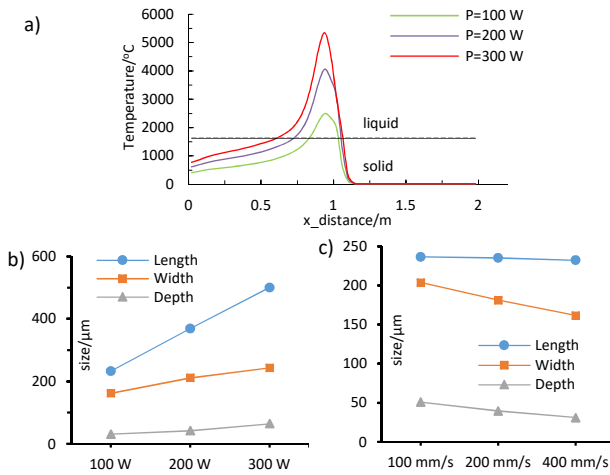## 3. Results and discussions

Figure 1. a) Longitudinal temperature profile. Melt pool dimensions for different values of b) laser powers and c) scan speeds.

Longitudinal temperature profiles for scan speed of 400 mm/s and three different values of laser input power have been plotted in **Figure 1 a**, and show that an increase in laser power can elevate the temperature to a large extent and produce longer melt pools. Length, width and depth of the melt pool for two additional sets of laser power and scan speed has been plotted in **Figure 1 b** and **c** respectively. It can be observed that decreasing the scan speed and increasing the laser power will expand the size of the melt pool in a non-isotropic manner.
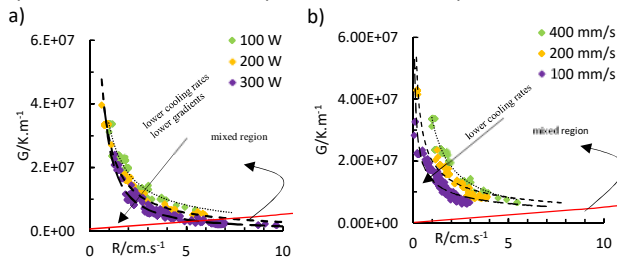

Figure 2. Grain morphology maps for a set of a) powers and b) speeds.

Solidification data, including temperature gradients, cooling rates and growth velocities, were determined on the borders of the melt pool at the start of solidification for different sets of laser powers and scan speeds (plotted in **Figure 2 a** and **b** respectively). In **Figure 2 a**, each color stands for a certain value of laser power. Increase in laser power reduces the average cooling rate, leading to coarser grain sizes as can be observed in **Figure 2 a**. Decrease in the laser scan speed has a similar impact on the cooling rate and thus the grain sizes. The discontinuous lines in **Figure 2 a** and **b** correspond to the curves of constant cooling rates, and thus based on the figure, lower cooling rates are predicted for higher laser powers and lower scan speeds.
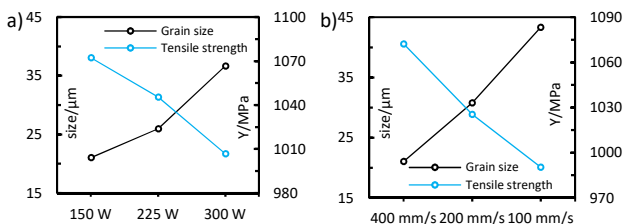

Figure 3. Effect of a) laser power and b) scan speed, on yield stress and average grain sizes.

Figure 3 a and **b** further validates the hypothesis that increased level of laser power and lower laser velocities result in bigger grain sizes. To evaluate the average size of grains, an empirical equation for rapid solidification (high cooling rates) of Ti6Al4V is implemented that relates cooling rate to β grain sizes [15]:

$$d(\mu m) = 3.1e^6 Cr(K.s^{-1})^{-0.93\pm0.1} \qquad (2)$$

where d is the grains size and Cr is the cooling rate. Additionally, to study the effect of grain sizes(d) on the yield strength (Y), a Hall-Petch like empirical equation for Ti6Al4V is used [16]:

$$Y\,(MPa) = 802.66 + 1236.5/\sqrt{(d(\mu m))} \qquad (3)$$

Figure 3 a and **b**, suggests that lower laser power along with higher laser speed ends in finer grains which consequently give rise to higher levels of tensile strength.

4. Conclusion

In this work a transient 3-D thermal model for SLM process for Ti6Al4V has been developed, which uses temperature-dependant thermal properties and takes phase transitions into account. Subsequently, based on the results of the thermal model, and for different values of laser power and scanning speed, grain morphology maps were drawn. These maps show that higher values of input power and lower values of scan speed result in lower cooling rates. According to rapid solidification models, such lower cooling rates cause the formation of coarser grains, giving rise to lower values of yield stress in the material. Future works will attempt at directly modelling the microstructure evolution, and then compare the results with corresponding experiments, to corroborate the findings.

References
[1] Li Y and Gu D, 2014. *Additive Manufacturing*, **1**, pp.99-109.
[2] Huang Y, Yang L.J, Du X.Z and Yang Y.P, 2016. *International Journal of Thermal Sciences*, **104**, pp.146-157.
[3] Antony K, Arivazhagan N and Senthilkumaran K, 2014. *Journal of Manufacturing Processes*, **16**(3), pp.345-355.
[4] Hussein A, Hao L, Yan C and Everson R, 2013. *Materials & Design*, **52**, pp.638-647.
[5] Gu D and He B, 2016. *Computational Materials Science*, **117**, pp.221-232.
[6] Zhang D.Q, Cai Q.Z, Liu J.H, Zhang L and Li R.D, 2010. The *International Journal of Advanced Manufacturing Technology*, **51**(5-8), pp.649-658.
[7] Li Y and Gu D, 2014. *Materials & Design*, **63**, pp.856-867.
[8] Shi Q, Gu D, Xia M, Cao S and Rong T, 2016. *Optics & Laser Technology*, **84**, pp.9-22.
[9] Criales L.E, Arısoy Y.M and Özel T, 2016. *The International Journal of Advanced Manufacturing Technology*, **86**(9-12), pp.2653-2666.
[10] Marimuthu S, Eghlio R.M, Pinkerton A.J and Li L, 2013. *Journal of Manufacturing Science and Engineering*, **135**(1), p.011004.
[11] Gürtler F.J, Karg M, Leitz K.H and Schmidt M, 2013. *Physics Procedia*, **41**, pp.881-886.
[12] Raghavan N, Dehoff R, Pannala S, Simunovic S, Kirka M, Turner J, Carlson N and Babu S.S, 2016. *Acta Materialia*, **112**, pp.303-314.
[13] Bontha S, Klingbeil N.W, Kobryn P.A and Fraser H.L, 2009. *Materials Science and Engineering*: A, **513**, pp.311-318.
[14] Mohanty S, Hattel J, 2014. *Physics Proceedia*, **56**, pp.379-389.
[15] Broderick T.F, Jackson A.G, Jones H and Froes F.H, 1985. *Metallurgical Transactions A*, **16**(11), pp.1951-1959.
[16] Sen I, Tamirisakandala S, Miracle D.B and Ramamurty U, 2007. *Acta Materialia*, **55**(15), pp.4983-4993.